J. Membrane Biol. 169, 13–27 (1999)

The Journal of
Membrane
Biology

Functional Analysis and Molecular Modeling of a Cloned Urate Transporter/Channel

E. Leal-Pinto[1], B.E. Cohen[2], R.G. Abramson[3]

[1]Division of Nephrology, Department of Medicine, Mount Sinai School of Medicine, Box #1243, One Gustave L. Levy Place, New York, NY 10029, USA

[2]Department of Anatomy and Cell Biology, Uniformed Services University School of Medicine, Building B, Room B2200, 4301 Jones Bridge Rd., Bethesda, MD 20819, USA

[3]Division of Nephrology, Department of Medicine, Mount Sinai School of Medicine, Box #1243, One Gustave L. Levy Place, New York, New York 10029, USA

Received: 13 October 1998/Revised: 28 January 1999

Abstract. Recombinant protein, designated UAT, prepared from a cloned rat renal cDNA library functions as a selective voltage-sensitive urate transporter/channel when fused with lipid bilayers. Since we previously suggested that UAT may represent the mammalian electrogenic urate transporter, UAT has been functionally characterized in the presence and absence of potential channel blockers, several of which are known to block mammalian electrogenic urate transport. Two substrates, oxonate (a competitive uricase inhibitor) and pyrazinoate, that inhibit renal electrogenic urate transport also block UAT activity. Of note, oxonate selectively blocks from the cytoplasmic side of the channel while pyrazinoate only blocks from the channel's extracellular face. Like oxonate, anti-uricase (an electrogenic transport inhibitor) also selectively blocks channel activity from the cytoplasmic side. Adenosine blocks from the extracellular side exclusively while xanthine blocks from both sides. These effects are consistent with newly identified regions of homology to uricase and the adenosine A1/A3 receptor in UAT and localize these homologous regions to the cytoplasmic and extracellular faces of UAT, respectively. Additionally, computer analyses identified four putative α-helical transmembrane domains, two β sheets, and blocks of homology to the *E* and *B* loops of aquaporin-1 within UAT. The experimental observations substantiate our proposal that UAT is the molecular representation of the renal electrogenic urate transporter and, in conjunction with computer algorithms, suggest a possible molecular structure for this unique channel.

Key words: Adenosine receptor — Transport — Channel — Urate — Galectin — Uricase

Introduction

The ubiquitous intracellular production of urate as a consequence of the metabolic degradation of the purines adenine and guanine in cells that contain xanthine oxidase [42] requires an efficient mechanism by which urate can exit cells to enter the extracellular compartment and be eliminated from the body. Although cellular efflux is essential to obviate intracellular crystallization of the poorly soluble urate [69], and therefore a critical first step in modulating urate homeostasis, the mechanism(s) responsible for egress of urate from cells has not been elucidated. The second step in the modulation of urate homeostasis is species dependent. In a large number of species a major fraction of extracellular (circulating) urate is transported into hepatocytes where it is degraded by the enzyme uricase within hepatic peroxisomes [17, 29, 46] to a highly water soluble product, allantoin, which is then eliminated by renal excretion [11]. In others, including man, birds, reptiles and some nonhuman primates, uricase is not expressed and urate is not further metabolized [3]. Whether an end product of purine metabolism in species lacking functional uricase or the residual, nonoxidized urate in species with hepatic uricase, extracellular urate is ultimately eliminated from the body and urate homeostasis is maintained via renal and, to a lesser extent, intestinal excretion [3, 61, 62]. Very limited information is available on the mechanism(s) by which urate is transported across intestinal epithelial cells [61, 62]. In contrast, the participation of the kidney in urate homeostasis and the mechanisms responsible for renal urate transport have been extensively examined [3]. In the multiple mammalian species studied, urate excretion represents the net effect of its free filtration at the glomerulus followed by both tubular reabsorption and

secretion that occur primarily within the convoluted and straight portions of the proximal tubule [3]. Mechanistically, two modalities of transport have been reported in renal cortical plasma membranes, an electroneutral urate/anion exchanger [10, 24, 25, 32–34, 57] and an electrogenic urate transporter [1, 2, 36, 57].

We have recently cloned a 1545 bp full-length cDNA that encodes a unique 322 amino acid protein, produced a 36–37 kDa recombinant protein from the coding region of this sequence, and functionally reconstituted a highly selective 10 pS voltage-sensitive urate transporter/channel (designated UAT) by fusion of this recombinant protein with lipid bilayers [40]. It is of note that a polyclonal antibody to affinity purified porcine uricase was used to identify the urate transporter/channel cDNA clone in a rat renal cDNA library [40]. This antibody was selected as a tool to clone this transporter based on a number of characteristics of the electrogenic urate transporter that resides in rat and rabbit renal cortical cell membranes [1, 2, 36]. First, the renal electrogenic urate transporter displays some similarities to the enzyme uricase [1, 2, 36, 37]. Second, hepatic uricase functions as a urate transporter when incorporated in proteoliposomes [54] and a highly selective urate channel when inserted in lipid bilayers [39]. Third, urate-binding protein affinity purified from rat renal cortical cell membranes on urate or xanthine agarose gels is highly immunoreactive to the polyclonal antibody to porcine uricase [37]. Fourth, this antibody specifically inhibits electrogenic urate transport in rat renal cortical membrane vesicles and finally, in immunocytochemical studies, anti-uricase is reactive in proximal tubules, the nephron site of urate transport [37]. Since the urate transporter/channel cDNA was not only identified with the polyclonal antibody to uricase, but the recombinant UAT protein was immunoreactive to anti-uricase and the antibody blocked urate channel activity in the lipid bilayer system [40], we proposed that this cDNA may be the molecular representation of the renal proximal tubule electrogenic urate transporter [1, 2, 36]. Based on the wide tissue distribution of the mRNA for this protein, we also postulated that this channel may serve an important "housekeeping" function to permit efflux of urate subsequent to its intracellular production [40].

Despite the above noted apparent similarities between recombinant UAT, the renal electrogenic urate transporter and the enzyme uricase, a data base search with the BLAST algorithms [5] failed to detect homology between UAT and uricase [40]. Rather, the amino and carboxy termini of UAT were noted to have varying degrees of homology to members of a family of cytoplasmic and secreted β galactoside binding proteins, the galectins [4, 8, 14, 21, 22, 26, 44, 51] while the intervening 61 amino acid sequence that links the amino and carboxy termini of UAT was found to be unique. It is of note that galectins had been postulated to participate in a variety of functions including cell migration, adhesion, regulators of cell proliferation, immune function, and neoplasia [4, 8, 14, 21, 22, 26, 44, 51], but none were previously considered to function as transport proteins. In the present studies we have obtained experimental evidence that supports our prior proposal that recombinant UAT does represent the molecular equivalent of the mammalian renal electrogenic urate transporter and have developed, and in part experimentally tested, a new molecular model of UAT. Importantly, although a data base search previously failed to report homology between the full-length sequence of UAT and uricase, a local block of homology to uricase has been detected within the unique 61 amino acid linker region of UAT. Moreover, other potentially important blocks of amino acids have been identified within this region of UAT including a domain which has homology to the adenosine/xanthine binding site of the A1 and A3 adenosine receptors, a domain with homology to the E loop of aquaporin-1 and a domain with homology to the B loop of this same protein. Thus, while UAT does appear to be a member of the galectin family, our data suggest that the unique linker domain is likely to play a critically important role in conferring transport/channel function on this novel protein.

Materials and Methods

Preparation of Recombinant Protein

As previously reported, recombinant protein was prepared from the cDNA that we cloned from a rat renal cDNA library [40]. In brief, the full-length of the coding sequence of UAT in pBluescript was amplified by PCR using a sense primer with a *Bam*HI site immediately 5′ to the start codon [5′-GCGGATCCATGGCTTTCTTCAGCACCCAG-3′] and an antisense primer with a *Pst*I site just 3′ to the stop codon [5′-GCCTGCAGCTAGGTCTGCACGTGTGTCAGC-3′]. The purified PCR product was subcloned into *Bam*HI and *Pst*I digested pRSETA (Invitrogen, San Diego, CA) for subsequent production of a fusion protein with a six-histidine metal chelating domain 5′ to the coding region of UAT. Following overnight growth of SURE cells (Stratagene, La Jolla, CA) that had been transformed with pRSETA-UAT, pRSETA-UAT was isolated (Qiagen Plasmid Maxi kit, Qiagen, Chatsworth, CA) and used to transform BL21(DE3)pLysE cells (Novagen, Madison, WI). Colonies of BL21(DE3)pLysE cells containing pRSETA-UAT were grown in Super media (Qiagen) until the optical density reached 0.6–0.7. Thereafter, isopropyl-1-thio-β-D-galactopyranoside (IPTG) was added to a final concentration of 0.4 mM, the culture was grown for an additional 4 hr and then centrifuged at 5,000 × *g* for 20 min in a Sorvall RC-5B refrigerated centrifuge (DuPont). Cell pellets were stored at −70°C until recombinant protein was isolated. Following cell lysis, the recombinant protein was harvested by metal affinity chromatography on a nickel chelating resin, Ni-NTA, (Qiagen) in the presence of denaturants (guanidine, urea), detergent (TritonX-100) and glycerol (10%) according to the Qiagen protocol for insoluble proteins. Protein containing eluate fractions were pooled, diluted to a protein concentration of 0.1 mg/ml and slowly dialyzed at 4°C to renature the protein. The concentration of urea in the dialyzed

eluate was progressively reduced from 8 to 0 mM, the NaCl concentration was progressively increased to 0.8 M, the pH was raised from 4.5 to 7.5 with Tris-HCl while the concentration of glycerol was maintained at 10%. The dialyzed eluate was aliquoted and stored at −70°C until used in the lipid bilayer experiments.

Functional Assessment of Recombinant UAT Protein

Proteoliposomes Preparation

Bovine brain phosphatidyl-ethanolamine (PE) and phosphatidylserine (PS) (Avanti Polar Lipids, Birmingham, AL), each at 10 mg/ml, were mixed in a ratio of 1:1 (wt/wt), evaporated to dryness under a stream of nitrogen and then suspended in 49 μl of 220 mM Cs_2SO_4 and 10 mM HEPES-NaOH at pH 7.4. Proteoliposomes were subsequently formed by sonicating the suspension of PE and PS with 1 μl of recombinant UAT protein for 30 sec at 80 kHz in a bath sonicator (Laboratory Supplies, Hicksville, NY) [39, 40]. New proteoliposomes were prepared for each experiment.

Lipid Bilayer Chamber, Formation of Lipid Bilayer and Channel Reconstitution

The bilayer chamber was identical to that previously reported [39, 40]. In all experiments both chambers of the plexiglass bilayer apparatus were initially filled with 1 ml of a solution containing 2.5 mM urate, 220 mM Cs_2SO_4, and 0.25 mM $CaCl_2$ that was buffered to pH 7.4 with 10 mM HEPES-NaOH. Thereafter, a 50 μm hole in a Teflon film (Type C-20, 12.5 μm thick, Dupont electronics, Wilmington, DE) that was sandwiched between the two cups of the chamber was painted with lipid using a club shaped glass rod. The lipid used for the bilayer consisted of a 1:1 mixture of PE and PS (each at 10 mg/ml) that had been dried under nitrogen and dissolved in decane (Sigma Chemical, St. Louis, MO) to a concentration approximating 50 mg lipid/ml. Junction potentials were corrected with the zero adjust system of the patch-clamp amplifier (Axopatch 200B, Axon Instruments, Burlingame, CA). Voltage was generated, clamped at varying levels (+100 to −100 mV), and controlled with the patch-clamp amplifier. When a stable resistance of at least 100 gigohms and a noise level of less than 0.1 pA were maintained the experiments were initiated by addition of 1 μl of the UAT-containing proteoliposomes to the trans chamber. The contents in the trans chamber were stirred (generally 2–3 min) until the proteoliposomes fused with the lipid bilayer. Fusion was detected by the onset of channel gating (clear transitions between the closed and open states).

Functional Analysis of the Channel

In each experiment channel activity was initially evaluated in the presence of symmetrical solutions of 2.5 mM urate in 220 mM Cs_2SO_4, 0.25 mM $CaCl_2$, and 10 mM HEPES-NaOH at pH 7.4. In one group of studies the channel was subsequently assessed after the solution in the trans chamber was replaced with 2.5 mM oxonate (Sigma Chemical). In the remaining studies the channel was subsequently examined in the presence of symmetrical 2.5 mM urate solutions, but after the trans or cis solution was pulsed with μl volumes of one of the following reagents to achieve progressively increased concentrations in the bath: 2.5 mM oxonate, 2.5 mM pyrazinoic acid (PZA, Aldrich Chemical, Milwaukee, WI), 1 mM adenosine (Sigma Chemical), 1 mM xanthine (Sigma Chemical), the IgG fraction of anti-porcine liver uricase (10 μg/ml). In some studies, channel activity was re-examined after the solution in the cis and/or trans chamber was replaced with a fresh urate containing, reagent-free solution. All reagents with the exception of the antibody were prepared in 220 mM Cs_2SO_4 and 10 mM HEPES-NaOH buffered to pH 7.4.

Data Collection and Analysis

Current output of the patch clamp was filtered at 1 kHz through an eight-pole Bessel filter (Model 902, Frequency Devices, Haverhill, MA) that was digitized at 2.5 kHz (Digi Data 1200 series Interface, Axon Instruments). Commercial software (pCLAMP, Version 7.0, Axon Instruments) was used for data analysis after additional digitized filtering at not less than 100 Hz.

Results

Voltage Sensitivity and Orientation of UAT in Lipid Bilayer

As previously reported, fusion of recombinant UAT with planar lipid bilayers results in reconstitution of a very selective 10 pS voltage sensitive urate channel [40]. As depicted, current traces obtained in symmetrical urate solutions at different holding potentials (Fig. 1*A* and *B*) reveal that the open probability of the urate channel is voltage dependent, being significantly greater at positive than negative voltages (Fig. 1*C*). This relationship between channel activity and voltage (Fig. 1) was very consistently observed in the present ($n = 34$) as well as prior series of experiments with recombinant UAT [40]. In view of the uniformity of response to a change in voltage, it appears that UAT inserts into the lipid bilayer in a specific direction. Based on the finding that protein insertion into cell membranes correlates directly with the anionic charge on membrane lipids [66], it is likely that the specific and consistent orientation of UAT in the bilayer similarly reflects the nonsymmetrical distribution of electrical charges on the bilayer lipids. In our bilayer system the cis side of the chamber simulates an intracellular compartment as this side of the chamber is exposed to changes in voltage: the cis side is connected to the voltage-holding electrode, with all voltages referenced to the trans (ground) side [39]. Since voltage sensors are generally believed to reside on the cytosolic side of channels in vivo [28], the voltage sensitivity of UAT implies that this channel is oriented in the bilayer with its voltage sensor and, therefore, its cytoplasmic domains facing the cis bilayer chamber. In this context, hyperpolarization (negative voltage) decreases and depolarization (positive voltage) increases UAT channel activity (Fig. 1).

Effect of Oxonate on the Activity of UAT

Since oxonate is both a potent inhibitor of electrogenic urate transport in rat and rabbit renal cortical membrane

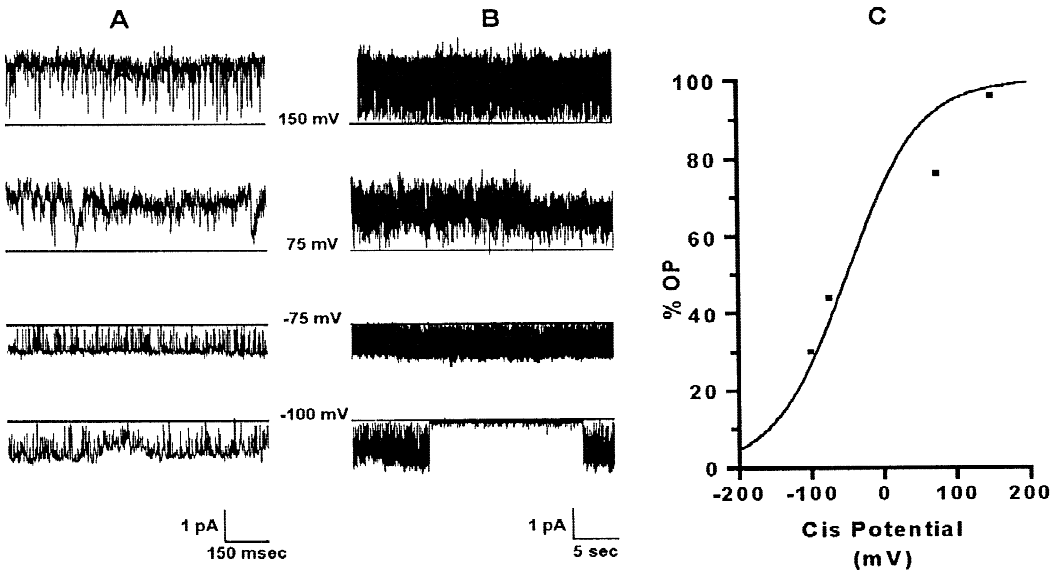

Fig. 1. Representative traces of UAT channel activity and open probability of the channel in symmetrical urate solutions. Channel activity was recorded in symmetrical urate solutions of 2.5 mM urate, 220 mM Cs_2SO_4, and 10 mM HEPES-NAOH at pH 7.4 following fusion of UAT containing proteoliposomes with the planar lipid bilayer. Solid horizontal lines in *A* and *B* depict the closed state. (*A*) Initial 5 sec of the 30 sec recordings of channel activity that are illustrated in *B* at different holding potentials in an individual experiment. (*C*) Open probability *vs.* voltage relationship of the channel shown in *B.*

vesicles [1, 2, 36] and a specific inhibitor of the enzymatic activity of uricase [20], the ability of oxonate to influence channel activity of recombinant UAT was assessed. In the presence of bi-ionic conditions, 2.5 mM oxonate trans and 2.5 mM urate cis, ($n = 3$), neither channel activity nor voltage sensitivity of the channel were initially influenced by the presence of 2.5 mM oxonate in the trans chamber (Fig. 2*A* and *B*). Importantly, however, in contrast to studies performed in symmetrical urate solutions (without oxonate) in which channel activity is detectable for many hours, in each experiment performed under these bi-ionic conditions channel activity ceased after approximately one hour (not depicted). The mechanism for this delayed blockade of channel activity was assessed by adding aliquots of the 2.5 mM oxonate solution to either the cis or trans chamber after channel activity was recorded in symmetrical urate solutions. As demonstrated in Fig. 2*C, D* and *E*, and as anticipated from the activity of the channel in the presence of 2.5 mM oxonate in the trans chamber (Fig. 2*A* and *B*), channel activity was not affected by 250 μM oxonate on the trans side of the channel. In contrast, open probability of the channel progressively decreased as the concentration of oxonate was sequentially increased on the cis side of the channel (Fig. 2*C, D* and *E*). Channel activity was 97% blocked at an oxonate concentration of 108 ± 16 μM (mean ± SE, $n = 3$) in the cis chamber. Of note, the oxonate induced block was reversed by replacing the oxonate containing solution in the cis chamber with oxonate-free solution (*not shown*). The asymmetrical effect of oxonate on channel activity implies that the delayed block that was observed under bi-ionic conditions resulted from accumulation of oxonate in the cis chamber consequent to oxonate's trans to cis flux through the channel. Based on the channel's orientation in the bilayer, this unilaterally induced block in channel activity also implies that oxonate interacts with a specific domain in UAT that is located on the cytoplasmic (cis) face of the channel whereas the extracellular domain(s) of UAT lack an oxonate binding site.

Effect of Pyrazinoate (PZA) on Activity of UAT

PZA is a well-known inhibitor of renal urate transport in vivo in multiple species [3] and, more specifically, a potent inhibitor of electrogenic urate transport in rat and rabbit renal cortical membrane vesicles [1, 2, 36]. In view of its affect on urate transport in intact renal membranes, the possibility was evaluated that PZA also interacts with recombinant UAT. PZA, like oxonate, induced a dose dependent block of urate channel activity (Fig. 3) that was reversed by replacing the PZA-containing solution in the chamber with fresh PZA-free urate solution (*not shown*). However, in distinct contrast to oxonate, PZA only induced a block in urate channel activity when present in the trans chamber: PZA completely blocked channel activity at a concentration of 24.1 ± 8.9 μM (mean ± SE, $n = 8$) in the trans chamber while as much as 100 μM PZA was without effect when

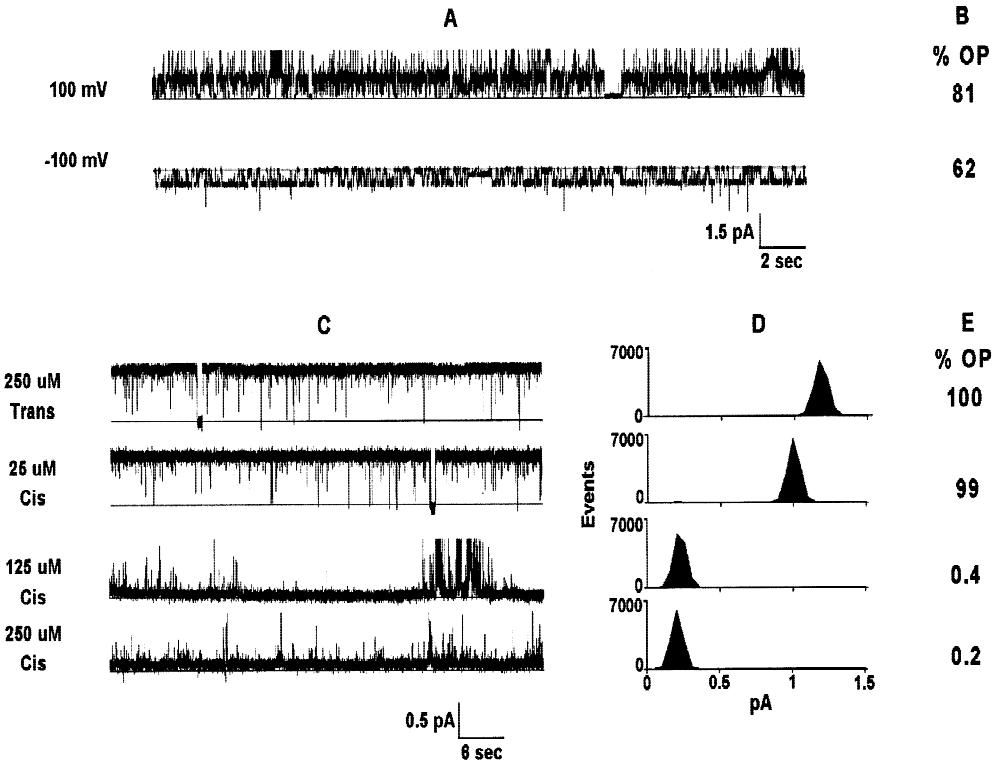

Fig. 2. Channel activity in the presence of oxonate. Solid horizontal lines in *A* and *C* depict the closed state. (*A*) 60-sec traces of channel activity in an individual experiment in the presence of bi-ionic conditions: 2.5 mM oxonate, 220 mM Cs_2SO_4, and 10 mM HEPES-NAOH at pH 7.4 in the trans chamber and 2.5 mM urate, 220 mM Cs_2SO_4, and 10 mM HEPES-NAOH at pH 7.4 in the *cis* chamber. (*B*) Open probability of the channel at +100 and −100 mV under bi-ionic conditions. (*C*) 60-sec traces of channel activity at a holding potential of +100 mV in symmetrical solutions of 2.5 mM urate, 220 mM Cs_2SO_4, and 10 mM HEPES-NAOH at pH 7.4 in the presence of the designated concentrations of oxonate in the trans chamber (upper trace) or cis chamber (lower 3 traces) in an individual experiment. (*D*) Histogram representation of the current and *E*, open probability of the channel for the specific conditions depicted in *C*.

added to the cis chamber. Based on the orientation of the urate channel in the lipid bilayer, the consistent unilateral trans effect of PZA implies that this agent interacts with a specific domain in UAT that is present on the extracellular (trans) face of the channel.

Identification of Local Block of Homology to Uricase within UAT

To understand the molecular basis for the very specific and localized sites of interaction of oxonate and PZA on the cytoplasmic and extracellular domains of the urate channel, respectively, (which could not be appreciated from our preliminary structural model of UAT [40]) the amino acid sequence of UAT was assessed with the multiple protein sequence alignment program MACAW [58] to search for local blocks of homology between UAT and a number of proteins whose structural organization have been reported. Since prior studies implied that there is some degree of homology between UAT and uricase [1, 2, 36, 37, 39, 40, 54], and oxonate which is a competitive inhibitor of uricase [20] blocked the reconstituted channel, a local block of homology to uricase was sought. As depicted in Fig. 4*A*, amino acid residues 151–185 of UAT shows 49% homology to residue 230–264 of porcine uricase [70] and 31% homology to residues 223–257 of Aspergillus uricase [41]. It is of note that Q228 in Aspergillus uricase, which is conserved in both UAT and porcine uricase, has been identified by x-ray crystallography as being critically important in the formation of the substrate-uricase complex [16]. Since oxonate is a competitive inhibitor of uricase [20], it seems likely that oxonate blocks urate channel activity by interacting within the region of UAT that has homology to uricase. Insofar as this assumption is correct, then this region of UAT must be accessible to oxonate from the cytoplasmic face of UAT.

Assessment of Local Block of Homology to Uricase with Anti-Uricase and Xanthine

Although the full-length cDNA sequence of UAT failed to demonstrate homology to uricase in a BLAST search,

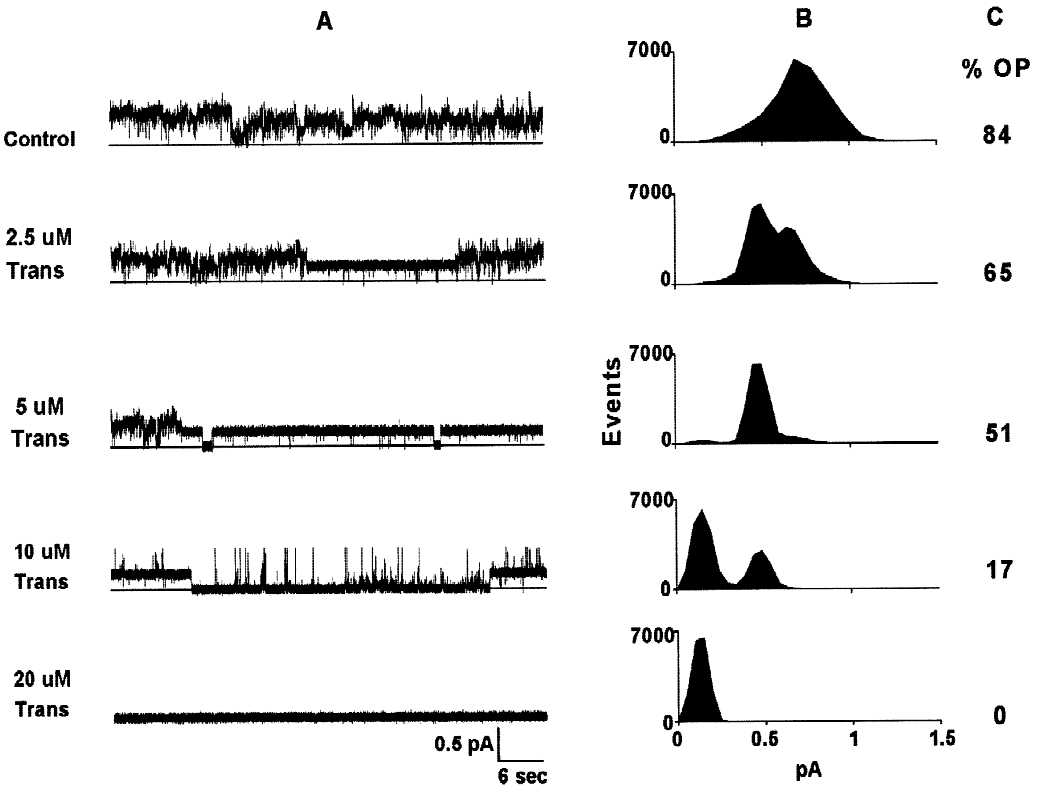

Fig. 3. Channel activity in the presence of pyrazinoate (PZA). Solid horizontal lines in *A* depict the closed state. (*A*) 60-sec traces showing multiple channels that were recorded in symmetrical solutions of 2.5 mM urate, 220 mM Cs_2SO_4, and 10 mM HEPES-NAOH at pH 7.4 in the absence (control) and presence of the designated concentrations of PZA in the *trans* chamber in an individual experiment at a holding potential of 25 mV. (*B*) Histogram representation of the current and *C*, open probability of the channel for the specific conditions depicted in *A*.

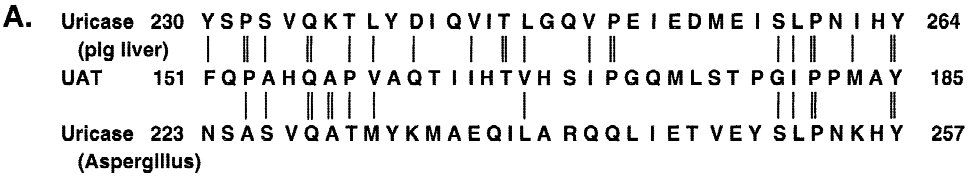

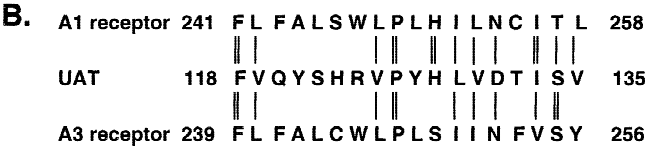

Fig. 4. Local blocks of homology in UAT to uricase and the adenosine A1/A3 receptor. (*A*) Alignment of UAT with porcine liver and Aspergillus uricase. (*B*) Alignment of UAT with the rat adenosine A1/A3 receptor. The residue number of the individual proteins is indicated at the beginning and end of each line. Double lines between amino acids indicate identical residues; single lines indicate homologous residues. Homology is defined according to the Swiss-Prot data bank in which amino acids in each of the following groups are homologous: [S, T, A, G, P]; [N, D, E, Q]; [R, K, H]; [M, L, I, V]; and [F, Y, W].

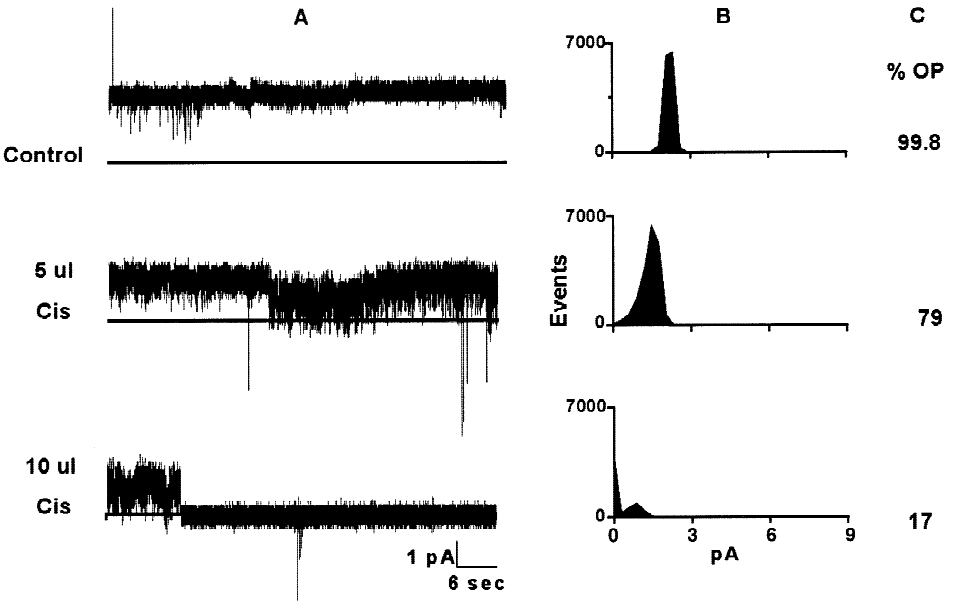

Fig. 5. Channel activity in the presence of anti-uricase. Solid horizontal lines in *A* depict the closed state. (*A*) 60-sec traces showing multiple channels that were recorded in symmetrical solutions of 2.5 mM urate, 220 mM Cs_2SO_4, and 10 mM HEPES-NAOH at pH 7.4 in the absence (control) and presence of anti-uricase in the *cis* chamber in an individual experiment at a holding potential of 25 mV. (*B*) Histogram representation of the current and *C*, open probability of the channel for the specific conditions depicted in *A*.

we previously demonstrated that the polyclonal antibody to uricase blocks urate channel activity [40]. In that study, however, antibody was applied to both the extracellular and cytoplasmic domains of UAT [40]. The present study demonstrates (Fig. 5) that urate channel activity is only blocked when the cytosolic domain of UAT (the cis chamber) is exposed to anti-uricase ($n = 3$): addition of up to twofold higher concentrations of anti-uricase to the extracellular side of UAT (*not shown*) fails to alter channel activity ($n = 3$). Nonimmune IgG was without effect when added to either side of the channel. Insofar as this antibody was made to affinity purified uricase [37] it is presumed that the antibody interacts with amino acids within the region of UAT that has homology to uricase. Thus, the single sided cytoplasmic effect of anti-uricase, like the single sided cytoplasmic effect of oxonate, implies that the domain within UAT that has homology to uricase resides, at least in part, on the cytoplasmic side of this protein.

Because xanthine and urate were equally effective as ligands to affinity purify urate binding proteins from rat renal plasma membranes [37], and xanthine is a competitive inhibitor of uricase [46], the effect of xanthine on urate channel activity was also evaluated. In contrast to the unilateral effects of anti-uricase and oxonate, xanthine blocked channel activity when present on either the extracellular or cytoplasmic side of UAT. Of interest, the concentration of xanthine (4.6 ± 1.5 μM, mean ± SE, $n = 5$) that was required to completely block channel activity when added to the extracellular side of UAT (Fig. 6) was approximately one-tenth that which blocked from the channels cytoplasmic face (*not shown*). These experiments are consistent with an interaction of xanthine with amino acids within the block of homology to uricase on the cytoplasmic side of UAT, but also indicate that an additional binding site with a higher affinity for xanthine is present within the extracellular domain of UAT.

Identification of Local Block of Homology to the Adenosine Receptor within UAT

Based on the observation that xanthine blocks channel activity from both the cytoplasmic and extracellular sides of UAT, local blocks of homology were also sought between UAT and proteins, other than uricase, with known xanthine binding sites. In this respect, it is well known that different xanthine derivatives are potent antagonists of A1 adenosine receptors [30]. As demonstrated in Fig. 4*B*, amino acid residues 118–135 of UAT have 61% homology to amino acids 241–258 of the rat A1 adenosine receptor [45] and 50% homology to residues 239–256 of the rat A3 adenosine receptor [71]. Importantly, it is in this region of the A1 and A3 receptors, specifically residues P249, H251 and N254 of the adenosine receptor that xanthine (and adenosine) bind [35, 52]. These amino acids of the A1 receptor align with P126, H128 and D131 of UAT (Fig. 4*B*). Figure 7 demonstrates that adenosine, like xanthine (Fig. 6), is a potent

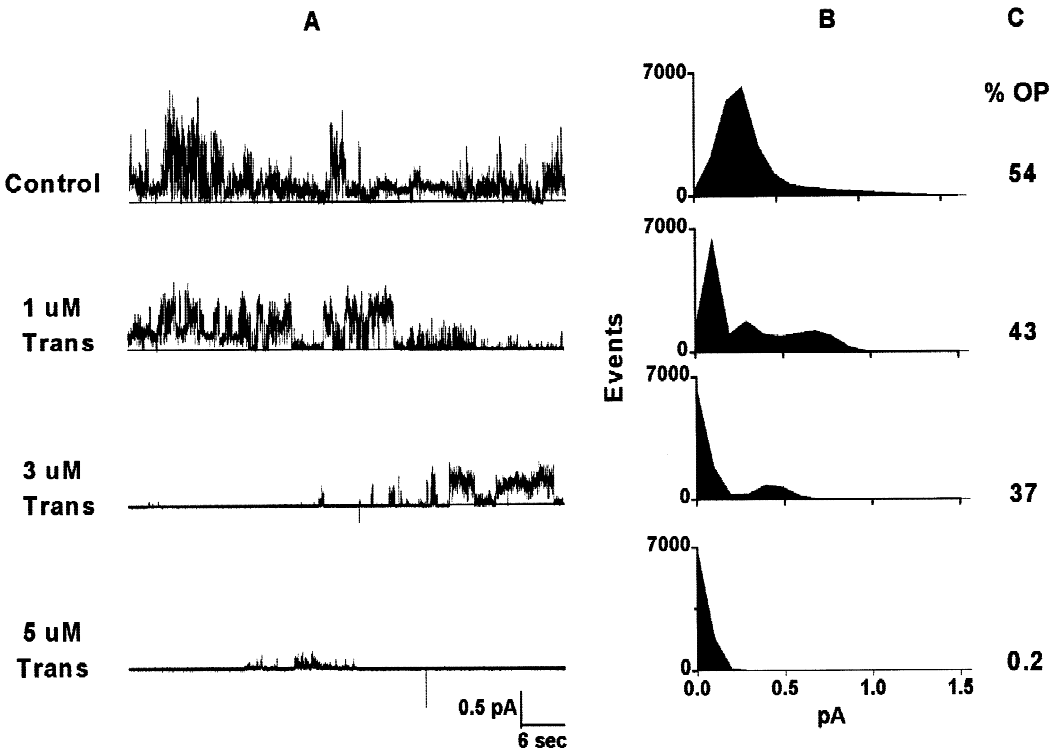

Fig. 6. Channel activity in the presence of xanthine. Solid horizontal lines in *A* depict the closed state. (*A*) 60-sec traces showing multiple channels that were recorded in symmetrical solutions of 2.5 mM urate, 220 mM Cs_2SO_4, and 10 mM HEPES-NAOH at pH 7.4 in the absence (control) and presence of the designated concentrations of xanthine in the trans chamber in an individual experiment at a holding potential of 25 mV. (*B*) Histogram representation of the current and *C,* open probability of the channel for the specific conditions depicted in *A.*

blocker of UAT channel activity when added to the extracellular side of the channel: a total block of channel activity was observed at an adenosine concentration of 4.6 ± 2.6 μM (mean ± SE, $n = 3$). However, in contrast to xanthine, adenosine failed to block channel activity when applied to the cytoplasmic domain of UAT ($n = 3$, not shown). Based on the unilateral effect of adenosine on channel activity, it is possible to localize the adenosine-like binding site in UAT, at least in part, to the extracellular domain of the protein. Since xanthine has a high affinity for the A1/A3 receptor, it is presumed that the block in channel activity that is induced by xanthine in the trans chamber is consequent to binding to amino acid residues within this extracellular domain of UAT.

Identification of Potential Membrane-Spanning Domains, Beta Sheets and a Region of Homology to the E and B loops of Aquaporin 1 in UAT

The above experimental data provides strong evidence that residues 118–135 of UAT (the region with homology to the adenosine receptor) must be separated from residues 151–185 (the region with homology to uricase) by a transmembrane domain. The program TopPred II [13] was used to determine if a hydrophobic domain is likely to span the membrane between these regions. In this regard the corresponding hydrophobicity profile of UAT, as calculated using the Kyte-Doolittle scale [38], clearly indicates the existence of a hydrophobic peak located between residues 128–148 (Fig. 8). Within this portion of UAT amino acids 125–145 of UAT are predicted to form an α-helix: this membrane spanning domain would connect the extracellular region of UAT that has homology to the A1/A3 receptor to the intracellular region that has homology to uricase. Of interest, this predicted α-helix has 38% homology (3 identical, 5 conserved amino acids) to the α-helix that has been documented by x-ray crystallography to form transmembrane domain E (residues 134–156, Fig. 9*A*) in bacterial rhodopsin [53]. This same region of UAT also has 30% homology (3 identical, 4 conserved amino acids) to the α-helix that is predicted to form transmembrane domain 3 (residues 162–184, Fig. 9*B*) of uric acid/xanthine permease, a fungal urate/xanthine transporter [23] that is otherwise unrelated to UAT.

Utilizing TopPred II, three additional α-helices are predicted in UAT: residues 15–35, 158–174 and 272–291: the hydrophobicity profile indicates that these are hydrophobic segments long enough to span the membrane (Fig. 8). It is of note that the putative transmem-

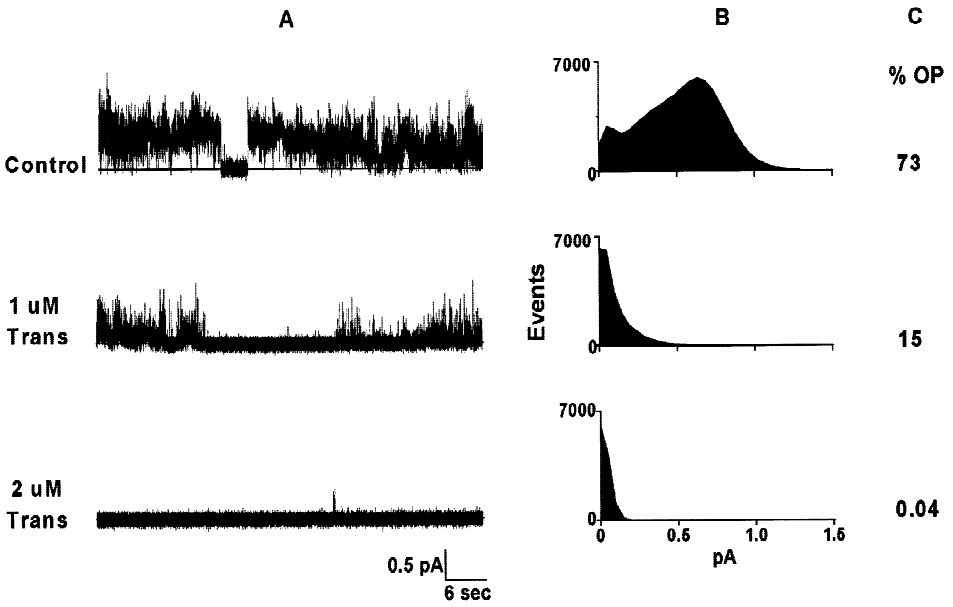

Fig. 7. Channel activity in the presence of adenosine. Solid horizontal lines in *A* depict the closed state. (*A*) 60-sec traces showing multiple channels that were recorded in symmetrical solutions of 2.5 mM urate, 220 mM Cs_2SO_4, and 10 mM HEPES-NAOH at pH 7.4 in the absence (control) and presence of the designated concentrations of adenosine in the trans chamber in an individual experiment at a holding potential of 25 mV. (*B*) Histogram representation of the current and *C,* open probability of the channel for the specific conditions depicted in *A.*

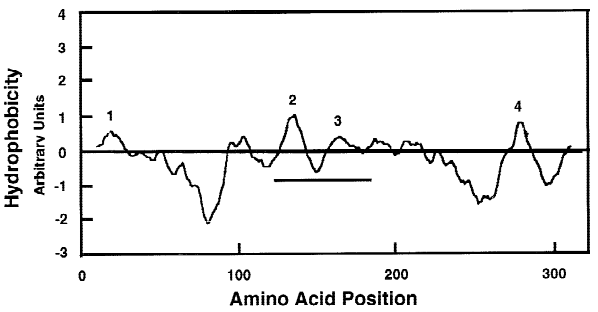

Fig. 8. Hydrophobicity profile of UAT as calculated by TopPred II using the Kyte-Doolittle scale. Numbers 1–4 represent hydrophobic peaks that form α-helices which are long enough to cross the membrane. The solid horizontal line delineates the unique 61 amino acid sequence that links the amino and carboxy termini of UAT.

brane domain composed of amino acids 15–35 has 52% homology (7 identical, 4 conserved amino acids) to the α-helix that is predicted to form transmembrane domain 2 (residues 133–153, Fig. 9*C*) in urate/xanthine permease [23] while amino acids 158–174 of UAT has 59% homology (3 identical, 7 conserved amino acids) to a portion of the α-helix that has been reported by x-ray crystallography to form transmembrane domain IX (residues 336–357, Fig. 9*D*) of subunit 1 of cytochrome C oxidase [64]. In addition to these four putative transmembrane α-helices, two β sheets are predicted in UAT encompassing amino acids 96–104 and 111–119 of UAT. These residues are long enough to traverse the membrane and, because both β sheets are amphiphilic, may represent a pore-like domain that can move in and out of the membrane [60].

Insofar as UAT functions as a transporter/channel, it seems relevant to note that the second and third putative transmembrane domains and the blocks of amino acids with homology to the A1/A3 adenosine receptor and uricase that are described above are all located in whole or in large part within the previously described 61 amino acids of UAT which was considered unique on the basis of a BLAST search [40]. Of note, using the program MACAW local blocks of homology have also been detected in this segment of UAT to the two loops of human aquaporin-1 that are believed to form the actual water channel [31]: amino acids 146–160 of UAT have 60% homology (4 identical, 5 conserved amino acids) to residues 186–200 that comprise loop E (Fig. 9*E*) and amino acids 170–184 of UAT have 53% homology (3 identical, 5 conserved amino acids) to residues 70–84 that form loop B in aquaporin-1 (Fig. 9*F*).

Discussion

We previously reported that a recombinant protein, UAT, which was prepared from a unique cDNA that was cloned from a rat renal library functioned as a highly selective voltage-sensitive urate transporter/channel in lipid bilayers [40]. Based in large part on the findings that anti-uricase specifically inhibits electrogenic urate

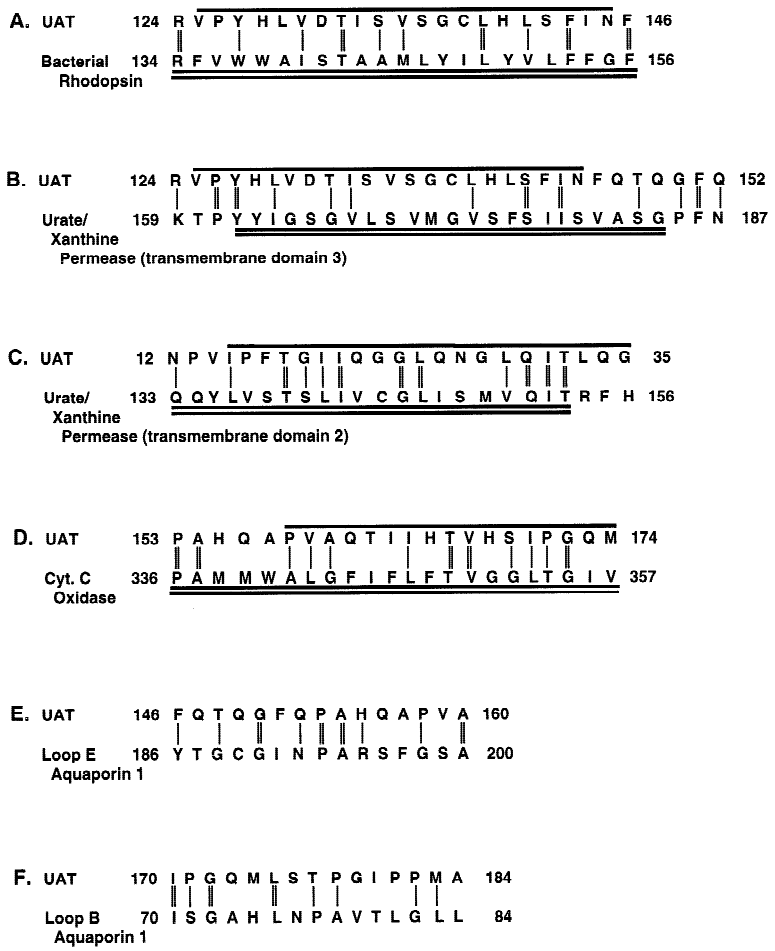

Fig. 9. Local blocks of homology in UAT to bacterial rhodopsin, urate/xanthine permease, cytochrome C oxidase and the E and B loops of aquaporin-1. (*A*) Alignment of UAT with transmembrane domain E of bacterial rhodopsin. (*B*) Alignment of UAT with transmembrane domain 3 of urate/xanthine permease. (*C*) Alignment of UAT with transmembrane domain 2 of urate/xanthine permease. (*D*) Alignment of UAT with transmembrane domain 9 of subunit 1 of cytochrome C oxidase. (*E*) Alignment of UAT with the E loop of aquaporin-1. (*F*) Alignment of UAT with the B loop of aquaporin-1. The residue number of the individual proteins is indicated at the beginning and end of each line. Double lines indicate identical residues; single lines indicate homologous residues as defined in Fig. 4. The single horizontal line above the sequences delineate the putative membrane spanning domain in UAT; the double horizontal lines below the sequences delineate the homologous membrane spanning domain in bacterial rhodopsin, urate/xanthine permease and cytochrome C oxidase.

uptake in renal membrane vesicles [37] and blocks channel activity of recombinant UAT [40], we hypothesized that this protein might be the molecular representation of the proximal tubular electrogenic urate transporter that resides in rat, rabbit and human kidney [1, 2, 36, 57]. Evidence is now provided to substantiate this hypothesis. First, oxonate, a substrate whose only reported functions are to competitively inhibit the enzyme uricase [20] and to inhibit renal electrogenic urate transport [1, 2, 36] blocks UAT channel activity (Fig. 2). Second, pyrazinoate (PZA) an inhibitor of renal urate transport in many species [3] and a reagent that has been documented to specifically inhibit renal electrogenic urate transport [1, 2, 36], also blocks UAT channel activity (Fig. 3). These findings, in conjunction with the prior [40] and current observation that anti-uricase interacts with and significantly blocks UAT channel activity (Fig. 5), imply that there is a high degree of homology, if not identity, between UAT and the renal electrogenic urate transporter.

Based on the voltage dependence of UAT and a consistent pattern of channel activity *vs.* voltage (Fig. 1) [40] we have presumed that the cis and trans sides of the channel in the bilayer system represent, respectively, the cytoplasmic and extracellular faces of UAT. Moreover, since oxonate and PZA demonstrate distinct sidedness in their ability to block channel activity it has been possible to define the domains in which these substrates act: the site of interaction between PZA and UAT has been localized to the extracellular domain of UAT (Fig. 3), while that of oxonate has been identified on the cytoplasmic face of the protein (Fig. 2). The specific amino acids involved in the interaction between PZA and UAT are currently unknown. However, as oxonate is a competitive inhibitor of uricase [20] it is likely that oxonate similarly competes with urate for binding at a specific site within UAT. Importantly, a local block of homology to uricase has been identified in UAT (Fig. 4*A*) which includes the amino acid (glutamine 228 of uricase) that has been defined in the crystal structure of uricase as

essential for substrate binding [16]. It is suggested that this glutamine may also represent the urate binding site in UAT and, as in the case of uricase, oxonate and urate may compete at this site in UAT. Insofar as these assumptions are correct, and oxonate only blocks channel activity when applied to the cytoplasmic face of UAT (Fig. 2), then the region of UAT with homology to uricase must reside on the cytoplasmic face of the protein. Localization of this uricase-like domain to the cytoplasmic side of UAT is consistent with the block in channel activity induced by addition of xanthine to the cis chamber: xanthine has an affinity for uricase that approximates that of urate [46] and the purine ring of 8-azaxanthine, a xanthine derivative, has been documented to anchor to glutamine 228 in uricase [16]. Similarly, the block in UAT activity provoked by anti-uricase when added to the cis, but not trans chamber supports the assignment of the uricase-like domain to the cytoplasmic face of UAT. Clearly, confirmation of these presumptions as well as the definition of the binding site of PZA remains to be determined.

The identification of a region of homology to uricase is important because it both localizes a binding site for urate (and oxonate, xanthine and anti-uricase) within UAT and provides a likely basis for several previously unexplained observations. The latter include the original finding that the renal electrogenic urate transporter possesses a number of functional "uricase-like" characteristics [1, 2, 36]. Moreover, the presence of a domain with homology to uricase within UAT is likely to explain, at least in part, (i) the immunoreactivity of rat renal plasma membranes [37], affinity purified rat renal plasma membrane urate-binding proteins [37] and recombinant UAT [40] to anti-uricase, (ii) the ability of this antibody to identify the UAT clone in a rat renal cDNA library [40], and (iii) the anti-uricase induced inhibition of urate uptake in renal membrane vesicles [37] and block of channel activity of recombinant UAT (Fig. 5).

An equally important site that has now been identified within UAT is the region of homology to the adenosine A1/A3 receptors (Fig. 4*B*). This is the same adenosine "receptor-like" domain which was previously identified in the CFTR chloride channel and that appears to be responsible for the high affinity binding of adenosine and different xanthine derivatives [15]. It is of interest that the interaction of adenosine with the adenosine A1 and A3 receptors is well known to be involved in the regulation of multiple physiologic functions, including the activity of a number of transporters [9, 12, 18, 19, 27, 43, 48, 49, 63]. Such regulation is indirect, having been ascribed to the coupling of extracellular adenosine binding and activation of its receptors with a signal transduction system that includes a G protein [18, 59], the turnover of phosphoinositide [27], changes in intracellular free calcium [6, 27, 50, 55], phospholipase C [59], diacylglycerol [59], protein kinase C [59], cAMP [6, 18, 50, 55, 63], nitric oxide [49] and cGMP [49]. Insofar as adenosine blocks UAT channel activity (Fig. 7) it seems possible that this inhibition of channel activity also represents a regulatory effect of adenosine. However, in contrast to the previously observed indirect regulatory effects of adenosine, it is suggested that the binding of adenosine to UAT may alter the conformation of this protein and thereby directly regulate UAT channel activity. Of note, the reduction in urate excretion that has been reported in human subjects in association with the systemic infusion of adenosine [7] suggests that adenosine also interacts with UAT (or its homologue) in the human kidney to play a role in the regulation of the renal urate secretory process, a function ascribed to the renal electrogenic urate transporter [1, 2, 36, 57].

The single-sided effectiveness of adenosine in blocking UAT channel activity (Fig. 7) has permitted assignment of the domain in UAT with homology to the adenosine A1/A3 receptors to the extracellular face of UAT. Designation of the domains with homology to the adenosine A1/A3 receptor and uricase to the extracellular and cytoplasmic sides of UAT, respectively, demands the presence of an intervening hydrophobic membrane-spanning domain. A block of amino acids (125–145) that is situated between these two domains is predicted to form a hydrophobic α-helix (Fig. 8) and, in support of the likelihood that this block traverses the membrane, this region of UAT has significant homology to transmembrane domain E (38%) in the crystal structure of bacterial rhodopsin (Fig. 9*A*) [53] and a predicted membrane-spanning domain (30%) in urate/xanthine permease (Fig. 9*B*) [23]. Based on the strong experimental evidence in support of a membrane-spanning domain in UAT (Figs. 2, 3, 5, 6, and 7) and the prediction of a hydrophobic α-helix with homology to membrane-spanning domains in two known intrinsic membrane proteins [23, 53] we conclude that amino acids 125–145 is a transmembrane domain within UAT.

Although not yet confirmed by experimental evidence three additional hydrophobic domains, amino acids 15–35, 158–174, and 272–291 are predicted in UAT that are long enough to span the membrane (Fig. 8). In support of the probability that these α-helices form transmembrane domains in UAT are the findings that two of these α-helices are highly homologous to transmembrane domains in known membrane proteins, transmembrane domain 2 of urate/xanthine permease (Fig. 9*C*) [23] and transmembrane domain IX in the crystal structure of subunit 1 of cytochrome C oxidase (Fig. 9*D*) [64].

We previously postulated that UAT contains a single transmembrane domain [40]. However, the experimental data and computer analysis obtained in the present study provides a rationale for a revised model of the molecular structure of UAT (*see* Fig. 10). In this new

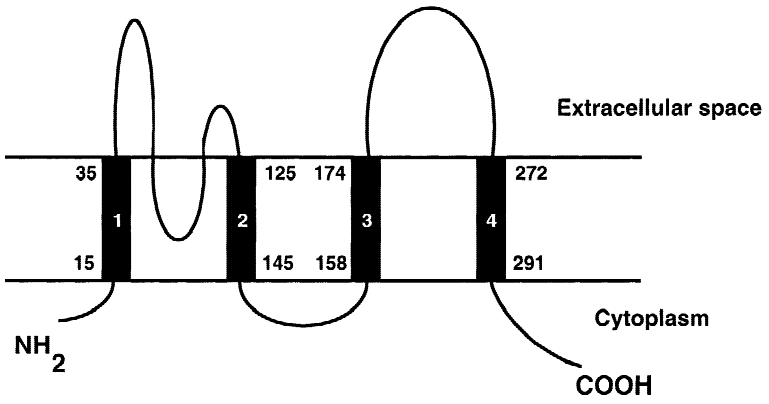

Fig. 10. Structural model of UAT. Numbers 1–4 designate transmembrane domains. Numbers adjacent to transmembrane domains indicate the amino acid residues at the beginning and end of each transmembrane domain. The "loop" into the membrane from the extracellular face of the protein designates the location of two β sheets that are connected by 6 amino acids that carry a net positive charge. The residues with homology to the A1/A3 receptor, uricase, and the E and B loops of aquaporin-1 are 118–135, 151–185, 146–160 and 170–184, respectively.

model UAT would have four membrane spanning domains with both the amino and carboxy termini located intracellularly (Fig. 10). Of note, in preliminary studies immortalized mammalian cells (LLC-PK1 cells) have been transfected with chimeric cDNAs that were constructed with the nucleotide sequence of the FLAG epitope on either the amino or carboxy terminus of UAT. In addition to finding that both constructs localize to the plasma membrane [56], a comparison of fluorescence of nonpermeabilized and permeabilized cells indicates that the amino and carboxy termini of UAT are both located on the cytoplasmic side of the membrane (*unpublished observations*). Thus, UAT must contain a minimum of two transmembrane domains. Although we currently favor the simplicity of a four transmembrane model in which the four α-helices in a single UAT molecule could encircle and thereby form a central stable hydrophilic pore-like structure within the membrane, rather than a more complex one in which several UAT molecules must isomerize to form a pore, it is evident that the definitive molecular structure for UAT remains to be elucidated.

It is of interest that UAT also contains blocks of amino acids with homology to the E and B loops of aquaporin-1 (Fig. 9*E* and *F*) [31]. Based on the above postulated model of UAT with 4 transmembrane domains, the region with homology to the E loop (amino acids 146–160) would be located in the cytoplasmic loop between transmembrane domains 2 and 3 of UAT while the domain with homology to the B loop (amino acids 170–184) would reside within the extracellular loop between transmembrane domains 3 and 4 (Fig. 10). In aquaporin-1 the extracellular E loop and intracellular B loop are postulated to dip into the membrane, meet within the membrane and form an hourglass-like structure that forms the pore of the water channel [31]. The amino acid motif asparagine, proline, alanine (NPA) in these loops is essential for the water permeability of aquaporin-1: mutation of N to Q in either loop E or B results in a marked reduction of water permeability [31]. Since alignment of UAT with the E loop of aquaporin-1 (Fig. 9*E*) reveals a QPA aligned with the NPA of aquaporin-1 and the region of UAT with homology to the B loop of aquaporin-1 does not contain an NPA motif (Fig. 9*F*), it is highly unlikely that UAT functions as a water channel. Rather, it seems possible that these homologous domains in UAT may participate in formation of the urate permeable pore within UAT in a manner that is analogous to the formation of the hourglass-like structure in aquaporin-1. Alternatively, the two β sheets (amino acids 96–104 and 111–109) that have been identified between transmembrane domains 1 and 2 on the extracellular face of UAT (Fig. 10) may participate in the formation of the pore in conjunction with the intracellular domain of UAT that has homology to loop E of aquaporin-1. Of interest, the six amino acids (105–110) that link the two β sheets carry a net positive charge (R, K, and E). Thus, independent of whether the β sheets directly participate in formation of the pore for urate, their mobility [60] may result in the presentation of this charged region to the cytoplasmic face of the molecule. Since voltage sensors are thought to reside on the cytoplasmic side of channels [28], this charged region may function as the voltage sensor in UAT. Alternatively, charged residues within the carboxy terminus of UAT may serve this function.

As previously reported [40] UAT exhibits homology with the galectins [4, 8, 14, 21, 22, 26, 44, 51], a family of β galactoside-binding proteins that have also been referred to as S-Lac lectins (soluble lactose-binding vertebrate lectins). At the time of our original description of UAT [40], galectins 1–5, 7 and 8 had been reported [4, 8, 14, 21, 22, 26, 44, 51]. Although multiple functions have been postulated for these galectins [4, 8, 14, 21, 22, 26, 44, 51], none have been considered as transport proteins. In fact, the galectins have been considered to be primarily cytoplasmic proteins that are sometimes externalized to the extracellular compartment [4, 8, 14, 21, 22, 26, 44, 51]. We previously noted that a major distinction between UAT and the other galectins is the unique 61 amino acid sequence that links the amino and carboxy termini of UAT and suggested that this region of the

protein might be important in allowing UAT to insert in the membrane and function as a urate channel [40]. Indeed, we now have evidence that this region of UAT is likely to play a very important role in imparting transport/channel function to this protein since this region contains the domains with homology to the adenosine A1/A3 receptor and uricase (Fig. 4) as well as the domains with homology to membrane-spanning components of other membrane proteins including transmembrane E of bacterial rhodopsin, transmembrane 3 of the urate/xanthine transporter, transmembrane IX of subunit 1 of cytochrome C oxidase, and the E and B loops of aquaporin 1 (Fig. 10).

Subsequent to our publication [40], galectin 9 was reported in mouse [67, 68], rat [67, 68] and humans [47, 65]: an additional, but unpublished sequence for a human intestinal galectin 9 isoform has also been deposited in GenBank (accession #AB006782). Using the BLAST algorithm for the local alignment of 2 sequences, the human (#Z49107 and #AB005894), mouse (#U55060) and rat (#U59462) galectin 9 nucleotide sequences are, respectively, 79, 89, and 99% identical to that of UAT (#U67958). Indeed, there is only one nucleotide difference between UAT and rat galectin 9. Rat and mouse galectin 9 have been postulated to play a role in thymocyte/epithelial interactions that are pertinent to thymic development [68] while human gelectin 9 has been suggested to play a role in cellular interactions of the immune system [65] and ecalectin (described as a variant of human galectin 9) is believed to be a selective eosinophil chemoattractant [47]. Although these galectins, like galectins 1–8, have been considered to be soluble proteins and not membrane proteins, as noted above UAT specifically localizes to plasma membranes in renal cell lines transfected with the cDNA for UAT [56]. As noted above, a previous BLAST search utilizing the linker region of UAT indicated that this region was unique [40]. Repetition of this search now reveals that the linker region of UAT is no longer unique: it is 98, 87 and 77% homologous to the linker regions of rat, mouse and human galectin 9, respectively. Based on the very high degree of homology in this important region of the protein, it seems likely that rat galectin 9 is, in fact, UAT and that the mouse and human homologues of UAT are also capable of transporting urate. Clearly, this possibility remains to be experimentally validated.

In summary, the present studies have provided experimental evidence that UAT is the molecular representation of the renal electrogenic urate transporter. In addition, based on experimental data as well as computer-generated analyses of blocks of amino acid sequence a new structural model of UAT with four transmembrane domains has been developed. It is appreciated that confirmation of this model will require the application of a number of additional experimental approaches such as mutagenesis and epitope tagging and, ultimately, the direct determination of the three dimensional structure of UAT.

This work was supported by National Institutes of Health grant DK52785 (R.G.A. and E.L-P.) and the Cystic Fibrosis Foundation (B.E.C.)

References

1. Abramson, R.G., King, V.F., Reif, M.C., Leal-Pinto, E., Baruch, S.B. 1982. Urate uptake in membrane vesicles of rat renal cortex. Effect of copper. *Am. J. Physiol.* **242:**F158–F170
2. Abramson, R.G., Lipkowitz, M.S. 1985. Carrier-mediated concentrative urate transport in rat renal membrane vesicles. *Am. J. Physiol.* **248:**F574–F584
3. Abramson, R.G., Lipkowitz, M.S. 1990. Evolution of the uric acid transport mechanisms in vertebrate kidney. *In:* Basic Principles in Transport, Vol. 3, R.K.H. Kinne, editor. pp. 115–153. Karger, Basel, Switzerland
4. Albrandt, K.A., Orida, N.K., Liu, F.-T. 1987. An IgE-binding protein with a distinctive repetitive sequence and homology with an IgG receptor. *Proc. Natl. Acad. Sci. USA* **84:**6859–6863
5. Altschul, S.F., Gish, W., Miller, W., Myers, E.W., Lipman, D.J. 1990. Basic local alignment search tool. *J. Mol. Biol.* **215:**403–410
6. Arend, L.J., Burnatowska-Hledin, M.A., Spielman, W.S. 1988. Adenosine receptor-mediated calcium mobilization in cortical collecting tubule cells. *Am. J. Physiol.* **255:**C581–C588
7. Balakrishnan, V.S., Coles, G.A., Williams, J.D. 1996. Effects of intravenous adenosine on renal function in healthy human subjects. *Am. J. Physiol.* **271:**F374–F381
8. Barondes, S.H., Cooper, D.N.W., Gitt, M.A., Leffler, H. 1994. Galectins: structure and function of a large family of animal lectins. *J. Biol. Chem.* **269:**20807–20810
9. Belardinelli, L., Shryock, J.C., Song, Y., Wang, D., Srivivas, M. 1995. Ionic basis of the electrophysiological actions of adenosine on cardiomyocytes. *FASEB J.* **9:**359–365
10. Blomstedt, J.W., Aronson, P.S. 1980. pH gradient stimulated transport of urate and ρ-aminohippurate in dog renal microvillus membranes. *J. Clin. Invest.* **65:**931–934
11. Briggs, J., Levitt, M.F., Abramson, R.G. 1977. Renal excretion of allantoin in rats: a micropuncture and clearance study. *Am. J. Physiol.* **233:**F373–F381
12. Casavola, V., Guerra, L., Reshkin, S.J., Jacobson, K.A., Verrey, F., Murer, H. 1996. Effect of adenosine on Na^+ and Cl^- currents in A_6 monolayers. Receptor localization and messenger involvement. *J. Membrane Biol.* **151:**237–245
13. Claros, M.G., von Heijne, G. 1994. TopPred II: an improved software for membrane protein structure predictions. *Comput. Appl. Biosci.* **10:**685–686
14. Clerch, L.B., Whitney, P., Hass, M., Brew, K., Miller, T., Werner, R., Massaro, D. 1988. Sequence of a full-length cDNA for rat lung beta-galactoside-binding protein: primary and secondary structure of the lectin. *Biochem.* **27:**692–699
15. Cohen, B.E., Jacobson, K.A., Kin, Y.-C., Huang, Z., Sorscher, E.J., Pollard, H.B. 1997. 8-cyclopentyl-1,3-dipropylxanthine and other xanthines differentially bind to the wild-type and ΔF508 mutant first nucleotide binding fold (NBF-1) domains of the cystic fibrosis transmembrnae conductance regulator. *Biochemistry* **36:**6455–6461
16. Colloc'h, N., El Hajji, M., Bachet, B., L'Hermite, G., Schiltz, M., Prangé, T., Castro, B., Mornon, J-P. 1997. Crystal structure of the

protein drug urate oxidase-inhibitor complex at 2.05 A resolution. *Nature Structural Biol.* **4:**947–952

17. De Duve, C., Baudhuin, P. 1966. Peroxisomes (microbodies and related particles). *Physiol. Rev.* **46:**323–357
18. Edwards, R.M., Spielman, W.S. 1994. Adenosine A1 receptor-mediated inhibition of vasopressin action in inner medullary collecting duct. *Am. J. Physiol.* **266:**F791–F796
19. Forrest, J.N., Jr. 1996. Cellular and molecular biology of chloride secretion in the shark rectal gland: regulation by adenosine receptors. *Kidney Int.* **49:**1557–1562
20. Fridovich, I. 1965. The competitive inhibition of uricase by oxonate and by related derivatives of *s*-triazines. *J. Biol. Chem.* **240:**2491–2494
21. Gitt, M.A., Massa, S.M., Leffler, H., Barondes, S.H. 1992. Isolation and expression of a gene encoding L-14-II, a new human soluble lactose-binding lectin. *J. Biol. Chem.* **267:**10601–10606
22. Gitt, M.A., Wiser, M.F., Leffler, H., Herrmann, J., Xia, Y.-R., Massa, S.M., Cooper, D.N.W., Lusis, A.J., Barondes, S.H. 1995. Sequence and mapping of galectin-5, a β-galactoside-binding lectin, found in rat erythrocytes. *J. Biol. Chem.* **270:**5032–5038
23. Gorfinkiel, L., Diallinas, G., Scazzocchio, C. 1993. Sequence and regulation of the uapA gene encoding a uric acid-xanthine permease in the fungus *Aspergillus nidulans. J. Biol. Chem.* **268:**23376–23381
24. Guggino, S.E., Martin, G.J., Aronson, P.S. 1983. Specificity and modes of the anion exchanger in dog renal microvillus membranes. *Am. J. Physiol.* **244:**F612–F621
25. Guggino, S.E., Aronson, P.S. 1985. Paradoxical effects of pyrazinoate and nicotinate on urate transport in dog renal microvillus membranes. *J. Clin. Invest.* **76:**543–547
26. Hadari, Y.R., Paz, K., Dekel, R., Mestrovic, T., Accili, D., Zick, Y. 1995. Galectin-8, a new rat lectin, related to galectin-4. *J. Biol. Chem.* **270:**3447–3453
27. Hayslett, J.P., Macala, L.J., Smallwood, J.I., Kalghatgi, L., Gasalla-Herraiz, J., Isales, C. 1995. Adenosine stimulation of Na^+ transport is mediated by an A1 receptor and a $[Ca^{2+}]i$-dependent mechanism. *Kidney Int.* **47:**1576–1584
28. Hille, B. 1992. *In:* Ionic Channels of Excitable Membranes 2nd Ed. Sinauer Associates, Sunderland, MA
29. Hruban, Z., Recheigl, M. 1969. Microbodies and related particles: morphology, biochemistry, and physiology. *In:* International Review of Cytology, Supplement 1. G.H. Bourne and J.F. Danielli, editors. pp. 20–39. Academic Press, New York
30. Jacobson, K.A., Van Galen, P.J.M., Williams, M. 1992. Adenosine receptors: pharmacology, structure-activity relationships, and therapeutic potentials. *J. Med. Chem.* **35:**407–422
31. Jung, J.S., Preston, G.M., Smith, B.L., Guggino, W.B., Agre, P. 1994. Molecular structure of the water channel through aquaporin CHIP: the hourglass model. *J. Biol. Chem.* **269:**14648–14654
32. Kahn, A.M., Aronson, P.S. 1983. Urate transport via anion exchange in dog renal microvillus membrane vesicles. *Am. J. Physiol.* **244:**F56–F63
33. Kahn, A.M., Branham, S., Weinman, E.J. 1983. Mechanism of urate and ρ-aminohippurate transport in rat renal microvillus membrane vesicles. *Am. J. Physiol.* **245:**F151–F158
34. Kahn, A.M., Shelat, H., Weinman, E.J. 1985. Urate and ρ-aminohippurate transport in rat renal basolateral vesicles. *Am. J. Physiol.* **249:**F654–F661
35. Kim, J., Wess, J., van Rhee, A.M., Shöneberg, T., Jacobson, K.A. 1995. Site-directed mutagenesis identifies residues involved in ligand recognition in the human A_{2A} adenosine receptor. *J. Biol. Chem.* **270:**13987–13997
36. Knorr, B.A., Beck, J.C., Abramson, R.G. 1994. Classical and channel-like urate transporters in rabbit renal brush border membranes. *Kidney Int.* **45:**727–736
37. Knorr, B.A., Lipkowitz, M.S., Potter, B.J., Masur, S.K., Abramson, R.G. 1994. Isolation and immunolocalization of a rat renal cortical membrane urate transporter. *J. Biol. Chem.* **269:**6759–6764
38. Kyte, J., Doolittle, R.F. 1982. A simple method for displaying the hydropathic character of a protein. *J. Mol. Biol.* **157:**105–132
39. Leal-Pinto, E., London, R.D., Knorr, B.A., Abramson, R.G. 1995. Reconstitution of hepatic uricase in planar lipid bilayer reveals a functional organic anion channel. *J. Membrane Biol.* **146:**123–132
40. Leal-Pinto, E., Tao, W., Rappaport, J., Richardson, M., Knorr, B.A., Abramson, R.G. 1997. Molecular cloning and functional reconstitution of a urate transporter/channel. *J. Biol. Chem.* **272:**617–625
41. Legoux, R., Delpech, B., Dumont, X., Guillemot, J.C., Ramond, P., Shire, D., Caput, D., Ferrara, P., Loison, G. 1992. Cloning and expression in Escherichia coli of the gene encoding Aspergillus flavus urate oxidase. *J. Biol. Chem.* **267:**8565–8570
42. Lehninger, A.L., Nelson, D.L., Cox, M.M. 1993. Biosynthesis of amino acids, nucleotide, and related molecules. *In:* Principles of Biochemistry, pp. 688–734, 2nd edition. Worth Publishers, New York
43. Ma, H., Ling, B.N. 1996. Luminal adenosine receptors regulate amiloride-sensitive Na^+ channels in A6 distal nephron cells. *Am. J. Physiol.* **270:**F798–F805
44. Madsen, P., Rasmussen, H.H., Flint, T., Gromov, P., Kruse, T.A., Honore, B., Vorum, H., Celis, J.E. 1995. Cloning, expression, and chromosome mapping of human galectin-7. *J. Biol. Chem.* **270:**5823–5829
45. Mahan, L.C., McVittie, L.D., Smyk-Randall, E.M., Nakata, H., Monsma, F.J., Jr., Gerfen, C.R., Sibley, D.R. 1991. Cloning and expression of an A1 adenosine receptor from rat brain. *Mol. Pharmacol.* **40:**1–7
46. Mahler, H.R., Baum, H.M., Hubscher, G. 1956. Enzymatic oxidation of urate. *Science* **124:**705–708
47. Matsumoto, R., Matsumoto, H., Seki, M., Hata, M., Asano, Y., Kanegasaki, S., Stevens, R.L., Hirashima, M. 1998. Human ecalectin, a variant of human galectin-9, is a novel eosinophil chemoattractant produced by T lymphocytes. *J. Biol. Chem.* **273:**16976–16984
48. McCoy, D.E., Schwiebert, E.M., Karlson, K.H., Spielman, W.S., Stanton, B.A. 1995. Identification and function of A1 adenosine receptors in normal and cystic fibrosis human airway epithelial cells. *Am. J. Physiol.* **268:**C1520–C1527
49. Miller, K.J., Hoffman, B.J. 1994. Adenosine A3 receptors regulate serotonin transport via nitric oxide and cGMP. *J. Biol. Chem.* **269:**27351–27356
50. Murthy, K.S., McHenry, L., Grider, J.R., Makhlouf, G.M. 1995. Adenosine A1 and A2b receptors coupled to distinct interactive signaling pathways in intestinal muscle cells. *J. Pharmacol. Exp. Ther.* **274:**300–306
51. Oda, Y., Herrmann, J., Gitt, M.A., Turck, C.W., Burlingame, A.L., Barondes, S.H., Leffler, H. 1993. Soluble lactose-binding lectin from rat intestine with two different carbohydrate-binding domains in the same peptide chain. *J. Biol. Chem.* **26:**5929–5939
52. Olaf, M.E., Ren, H., Ostrowski, J., Jacobson, K.A., Stiles, J.L. 1992. Cloning, expression, and characterization of the unique bovine A1 adenosine receptor. Studies on the ligand binding site by site-directed mutagenesis. *J. Biol. Chem.* **267:**10764–10770
53. Pebay-Peyroula, E., Rummel, G., Rosenbusch, J.P., Landau, E.M. 1997. X-ray structure of bacteriorhodopsin at 2.5 angstroms from microcrystals grown in lipidic cubic phases. *Science* **277:**1676–1682

54. Pordy, W.T., Lipkowitz, M.S., Abramson, R.G. 1987. Evidence for the transport function of uricase, an oxidative enzyme. *Am. J. Physiol.* **253:**F702–F711
55. Prie, D., Friedlander, G., Coureau, C., Vandewalle, A., Cassingena, R., Ronco, P.M. 1995. Role of adenosine on glucagon-induced cAMP in a human cortical collecting duct cell line. *Kidney Int.* **47:**1310–1318
56. Rappoport, J.Z., Lipkowitz, M.S., Mirshahi, T., Logothetis, D.E., Abramson, R.G. 1998. Cellular localization of a cloned urate transporter/channel. *J. Am. Soc. Neph.* **9:**56*A* (*Abstr.*)
57. Roch-Ramel, F., Werner, D., Guisan, B. 1994. Urate transport in brush-border membrane of human kidney. *Am. J. Physiol.* **266:**F797–F805
58. Schuler, G.D., Altschul, S.F., Lipman, D.J. 1991. A workbench for multiple alignment construction and analysis. *Proteins* **9:**180–190
59. Schwiebert, E.M., Karlson, K.H., Friedman, P.A., Dietl, P., Spielman, W.S., Stanton, B.A. 1992. Adenosine regulates a chloride channel via protein kinase C and a G protein in a rabbit cortical collecting duct cell line. *J. Clin. Invest.* **89:**834–841
60. Slatin, S.L., Qui, X.Q., Jakes, K.S., Finkelstein, A. 1994. Identification of a translocated protein segment in a voltage-dependent channel. *Nature* **371:**158–161
61. Sorenson, L.B. 1960. The elimination of uric acid in man studied by means of C^{14}-labeled uric acid. Uricolysis. *Scand. J. Clin. Lab. Invest.* **12:**(Suppl. 54) 1–214
62. Sorenson, L.B. 1978. Extrarenal disposal of uric acid. *In:* Uric Acid, Handbook of Experimental Pharmacology, Vol. 51. W.N. Kelley and I.M. Weiner, editors. pp. 325–336. Springer-Verlag, Berlin, Germany
63. Takeda, M., Yoshitomi, K., Imai, M. 1993. Regulation of Na(+)-$3HCO_3$-cotransport in rabbit proximal convoluted tubule via adenosine A1 receptor. *Am. J. Physiol.* **265:**F511–F519
64. Tsukihara, T., Aoyama, H., Yamashita, E., Tomizaki, T., Yamaguchi, H., Shinzawa-Itoh, K., Nakashima, R., Yaono, R., Yoshikawa, S. 1996. The whole structure of the 13-subunit oxidized cytochrome c oxidase at 2.8 A. *Science* **272:**1136–1144
65. Türeci, Ö., Schmitt, H., Fadle, N., Pfreundschuh, M., Sahin, U. 1997. Molecular definition of a novel human galectin which is immunogenic in patients with Hodgkin's disease. *J. Biol. Chem.* **272:**6416–6422
66. van Klompenburg, W., de Kruijff, B. 1998. The role of anionic lipids in protein insertion and translocation in bacterial membranes. *J. Membrane Biol.* **162:**1–7
67. Wada, J., Kanwar, Y.S. 1997. Identification and characterization of galectin-9, a novel β-galactoside-binding mammalian lectin. *J. Biol. Chem.* **272:**6078–6086
68. Wada, J., Ota, K., Kumar, A., Wallner, E.I., Kanwar, Y.S. 1997. Developmental regulation, expression, and apoptotic potential of galectin-9, a β-galactoside binding lectin. *J. Clin. Invest.* **99:**2452–2461
69. Wilcox, W.R., Khalaf, A., Weinberger, A., Kippen, I., Klinenberg, J.R. 1972. Solubility of uric acid and monosodium urate. *Mol. & Biol. Eng.* **10:**522–531
70. Wu, X.W., Lee, C.C., Muzny, D.M., Caskey, C.T. 1989. Urate oxidase: primary structure and evolutionary implications. *Proc. Natl. Acad. Sci. USA* **86:**9412–9416
71. Zhou, Q.Y., Li, C., Olah, M.D., Johnson, R.A., Stiles, G.L., Civelli, O. 1992. Molecular cloning and characterization of an adenosine receptor: the A3 adenosine receptor. *Proc. Natl. Acad. Sci. USA* **89:**7432–7436